

Influence of Microstructural Evolution Processed by ECAP on Corrosion Behavior of Pure Magnesium in RPMI-1640 Medium

Taito Hosaka¹, Iman Amanina¹, Naohiro Saruwatari¹, Shoichiro Yoshihara¹
and Bryan J. MacDonald²

¹*Department of mechanical Engineering, University of Yamanashi, 4-3-11, Takeda, Kofu-city, Yamanashi, Japan*

²*School of Manufacturing and Mechanical Engineering, Dublin City University, Dublin 9, Ireland*

Keywords: Microstructural Evolution, ECAP Process, Corrosion Behaviour, Pure Magnesium, RPMI 1640 Medium, Biomaterial.

Abstract: Influence of microstructure changes caused by Equal-channel angular pressing (ECAP) process on corrosion behavior of pure magnesium in RPMI-1640 medium was investigated. The grain size of ECAPed samples (30 μ m) were greatly reduced compared with the grain size of the annealed sample (200 μ m). Then, the immersion test has been carried out for a certain period of time. It was revealed that mass loss of the ECAPed sample is larger than the as-received sample and the annealed sample. Thus, it could be considered that many crystal defects yielded by ECAP process reduced the corrosion resistance. However, the corrosion resistance has been improved to a certain extent according to reduction of crystal defects through the heat treatment at the recrystallization temperature or lower. In addition, the amount of gas generation of the ECAP sample after immersion test is larger compared with the as-received sample. Therefore, correlation between the amount of gas generated and the mass loss was confirmed. Based on qualitative identification of the elements by Energy Dispersive X-ray Spectrometry (EDS), the corrosion products of the sample surface after the immersion test has been estimated to be a kind of calcium phosphate. These above results have indicated the potential for fabrication of magnesium as bioabsorbable materials.

1 INTRODUCTION

Magnesium (Mg) is present in high concentrations in sea water and the eighth most abundant element on the earth. It has also excellent specific strength and low density, only two-thirds that of Aluminum. Then, Mg and its alloys could be adopted in many applications including computer parts, mobile phones, aerospace components and handheld tools (Wu, 2007).

Mg alloys are also potentially useful for bone implants and stent applications due to their low density, inherent biocompatibility, adequate mechanical properties and fracture toughness higher than that of ceramics (Mani, 2007). Additionally, the elastic modulus of Mg alloys (40–45GPa) is closer to that of human bones (10–40GPa) than other commonly used implant materials such as Titanium (106GPa). Eventually, the stress-shielding phenomena caused by current metallic implants made of stainless steel or Titanium alloy could be minimized (Xu, 2007).

Another advantage of Mg in relation to other metallic implants is the degradability of Mg alloys which offers the possibility of repair and reconstruction of vascular compliance with minimum inflammatory response (Loos, 2007).

In recent years, the application of bioabsorbable materials for medical implants has drastically increased (Busch, 2014). Since magnesium is an essential element in our body, it can be absorbed into the body without leaving any harm. Therefore, many studies have been focused on using magnesium and its alloys for medical devices such as bioabsorbable stents (Hiromoto, 2012).

Nowadays, the traditional permanent metallic materials for the stents are modernly manufactured from stainless steel (316L), nitinol and cobalt-chromium alloys which have high corrosion resistance and remain as a permanent implant in the body. Thus, many limitations such as risk of chronic irritation caused by released toxic substances which might appear after long-term placement of the stents.

Magnesium is able to overcome many of these limitations since it could be absorbed into the body. For the patients with the coronary artery disease, the magnesium stents could temporarily function as a scaffold for supporting the vascular stenosis. The disappearance of the magnesium alloys stent is necessary after 6-12 (Werkhoven, 2011) months period. Therefore, the structural integrity of the implanted stent has to be preserve until the surgical region has completely heal, hence the corrosion behaviour of Mg and its alloys have received attention in recent years. However, study on the degradation behaviour and mechanisms of magnesium and its alloys in physiological environment such as inside the human body have not been elucidated.

The main factors affecting the corrosion performance of metallic materials as bioabsorbable stent include internal factors which are all about the material itself such as microstructure, distortion, surface condition and external factors such as influence of blood flow, body temperature and pH value. The effect of grain refinement by various severe plastic deformation methods on the corrosion behaviour of materials has caught much attention in recent years. During the last decade, equal-channel angular pressing (ECAP) has considered as the most appropriate procedure for the fabrication of ultrafine-grained (UFG) metals and alloys for industrial application. It has been widely-known that ECAP process significantly affects the mechanical properties of magnesium and its alloys. Although many studies have been done on the materials processed by ECAP, their corrosion resistance has been rarely reported (Song, 2010). The present work focused on the influence of microstructure change on corrosion resistance of pure Mg processed by ECAP.

Therefore, in this study, we attempted to investigate the immersion test on ECAPed pure Mg in RPMI 1640 medium. The results would be helpful for better understanding the corrosion behaviours of ECAPed pure Mg and its alloys, and explore their possibility for engineering applications.

2 EXPERIMENTAL

2.1 ECAPed Specimen Preparation

The specimen used for ECAP process was cut from the extruded pure Mg round bar (99.96%). The schematic illustration of the ECAP process is shown in Fig.1. The billets of the specimen for ECAP with

the size of diameter $\Phi 6$ mm \times length 50 mm were annealed for 24 hours at 723 K after cutting process. Then, the billets were repeatedly pressed for 4 times with a plunger speed of 4 mm/s at 573 K. Molybdenum disulfide as lubricant was used to reduce the friction coefficient between the billet and the die inner wall. During the each pressing process, the billet was inverted, and then rotated by 90° to the circumferential direction.

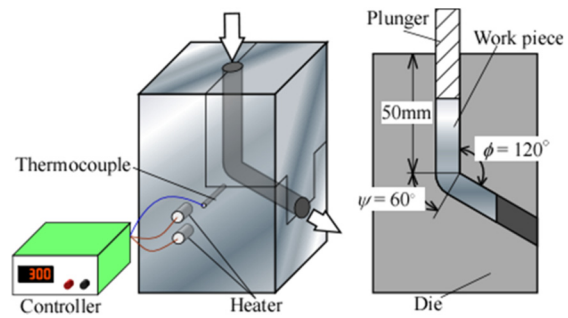


Figure 1: Schematic of ECAP process.

2.2 Experimental Conditions

Table 1 shows the kind of the samples on several experimental conditions of the different material types and the subsequent annealing times. Type (a) shows the ECAPed pure magnesium sample, type (b) the extruded (as-received) pure Mg sample and type (c) the annealed at 723 K for 24 hours pure Mg sample have been studied in comparison with the several conditions. Furthermore, the subsequent annealing process below the re-crystallization temperature was applied to ECAPed samples in order to verify the effect of crystalline defects on weakening pure Mg's corrosion resistance without increasing grain sizes. It has been processed at 423K for type (d) 2hours, type (e) 4hours and type (f) 6hours respectively to confirm the influence of the difference conditions on processing time. Besides, Park has reported that the subsequent annealing process could release the strain energy and weaken deformation texture of ECAPed samples (Park, 2008).

2.3 Microstructure Observation

The samples, used for optical microstructure observation were cut on perpendicular to the pressing direction from the ECAPed billet, and polished with distilled water and etched with acetic picral (100 ml 6 wt.% picric acid, 28.8 ml 99.7 wt.% acetic acid and 10 ml distilled water). Optical microscopy (NICON ECLIPSE MA200, Japan) and

Table 1: Samples on difference conditions of Mg.

| | Material type | Subsequent aging temp. [K] | Subsequent aging time[hrs] | Number of times of ECAP processing | ECAP speed [mm/s] |
|-----|-----------------------|----------------------------|----------------------------|------------------------------------|-------------------|
| (a) | ECAPed | - | 0 | 4 | 4 |
| (b) | As-received | - | - | - | - |
| (c) | Annealed (at 723K) | - | - | - | - |
| (d) | ECAP+ subsequent aged | 423 | 2 | 4 | 4 |
| (e) | ECAP+ subsequent aged | | 4 | | |
| (f) | ECAP+ subsequent aged | | 6 | | |

scanning electron microscope (JEOL JSM-6500F, Japan) equipped with the Electron Back Scatter Diffraction (EBSD) (EDAX) camera were adopted to observe the microstructures and more details of the samples.

The samples for EBSD were also cut perpendicular to the pressing direction, polished on the emery papers and buffing with the abrasive diamond solutions of particle size 1µm and 0.25µm. Afterward, they were etched with the solution of 10ml HNO₃, 30ml acetic acid, 40ml H₂O and 120ml ethanol for around 10s.

2.4 Microhardness Tests

The Vickers hardness test was carried out to investigate the mechanical properties of the samples. Vickers hardness measurements were performed using micro-hardness testing device (AKASHI MVK-G3500AT, Japan). The samples were cut from billets perpendicular to the pressing direction and polished. Measurements were carried out at least five times for each sample. The load of Vickers indenter was 25g.

2.5 Corrosion Tests

The corrosion behaviour of the ECAPed pure Mg was investigated by the immersion test for certain period. ECAPed samples used were cut from the core of the ECAPed billets, cleaned and polished to avoid the surface contamination of lubricant and so forth. The surface of all specimens was polished with #2000 grits emery paper to ensure the same surface roughness, and then cleaned in acetone by ultrasonic washing machine. The Size of the test sample was diameter Φ6mm × thickness 3mm, respectively. RPMI 1640 medium (Sigma-Aldrich R8758, Japan) as a corrosion solution was used for immersion test in all experiments to simulate the

internal environment. The temperature of the corrosion solution was 310K constant. In this study, Fetal Bovine Serum (FBS) was not added to the medium. The initial samples were polished with emery papers up to #2000 grits and cleaned. The measuring procedure of the polished samples was weighed at first, immersed in RPMI1640 medium (pH=7.4) for various intervals in corrosion test, cleaned with a corrosion product removal solution (20g CrO₃ + 2g Ba (NO₃)₂ + 1g AgNO₃ + 100ml Distilled water) after corrosion test, washed with acetone and weighed without corrosion product. The above steps were repeated and the mass loss in every interval was measured to evaluate the corrosion rate of ECAPed samples [g/m²]. Mass loss was obtained by the following equation.

$$ML = (W_0 - W) / S \tag{1}$$

where, W_0 [g] is mass of the sample before corrosion. W [g] is mass of after corrosion. S [m²] is Initial surface area of the sample.

Moreover, Changes in the pH value in the immersion test was recorded for 7 days.

In addition, the surface of the ECAPed sample after the immersion test for 24 hours was observed to identify the corrosion products. After the immersion test, the sample was rinsed with distilled water quickly, and dried to observe their surface by an optical microscope. The surface of the sample was analyzed by the energy dispersive X-ray spectroscopy (EDS) with the scanning electron microscope (Japan electron JSM-7100F).

Furthermore, the immersion test for 24 hours of ECAPed sample and As-received sample was conducted to measure the amount of generated gas with the corrosion test of the pure magnesium in RPMI 1640 medium. Fig.2 shows the method of immersion test.

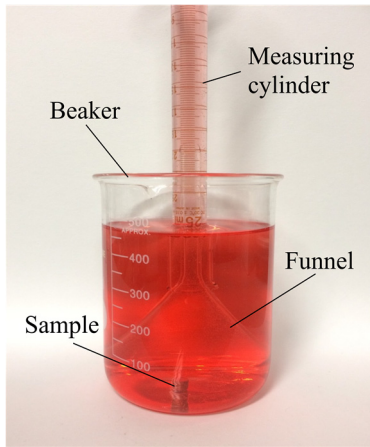


Figure 2: Photograph of immersion experiment.

3 RESULTS AND DISCUSSION

3.1 Microstructures of ECAPed Pure Mg Samples

Fig. 3(a)-(f) indicates the optical microstructures of the as-received, the annealed, the ECAPed, the subsequent aging for 2, 4 and 6 hours of the pure magnesium samples. The average grain size distribution before ECAP is around $200\mu\text{m}$. Thus, after the ECAP process, the average grain size distribution of $30\mu\text{m}$ was reduced. It is noteworthy that some larger grains are surrounded by some much smaller grains in the deformed microstructures. This phenomenon might be resulted from dynamic recrystallization since the temperature (at 573K) of ECAP process is higher than the recrystallization temperature of Mg.

Fig.4(a)-(f) shows the inverse pole figure map of these samples also. In comparison with the as-received, the crystal orientation of ECAPed sample

has significantly changed. Thus the effect of the shear stress applied into the material could be confirmed.

Fig. 5(a)-(f) shows the image quality map by EBSD of these samples. The polishing method of the sample in EBSD was all the same approach. Hence, it was considered that there is no difference in strain applied to the surface of each sample by the polishing. The crystalline of the ECAPed sample was considered low compared to the untreated sample and the annealed sample.

On EBSD, The factor affecting the quality of diffraction patterns in a materials science standpoint is the perfection of the crystal lattice in the sample. Thus, any distortions to the crystal lattice of the sample would be produced to the lower quality (more diffuse) diffraction patterns. It enables the Image quality (IQ) parameter to be used to give a qualitative description of the strain distribution.

As seen in figure (a), (b) and (c), the ECAP sample is confirmed to be less crystalline in comparison with the as-received sample and the annealed sample. It could be considered that ECAP process increases the crystal defects of the material by introducing a shear strain to the material at the bent portion of the die and refining the grains.

In addition, from figure (a), (d), (e) and (f), the crystalline of the subsequent aged sample was slightly increased. Hence, it could be concluded that crystal defects such as dislocation and strain of ECAPed sample was recovered by subsequent annealing from ECAP.

3.2 Microhardness Test

Fig. 6(a)-(f) shows the Vickers hardness results. Compared to the as-received samples and the annealed samples, the ECAP processed samples

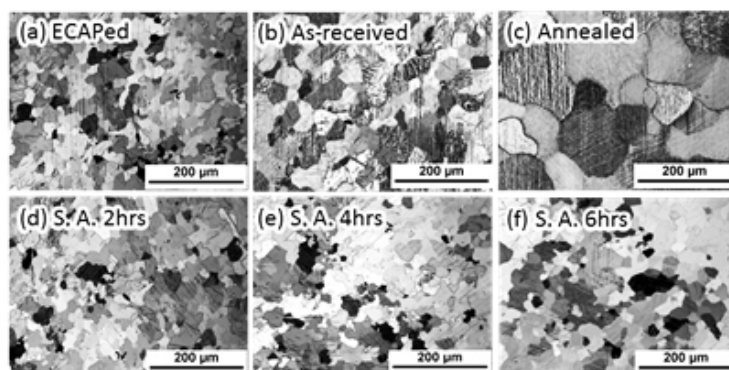


Figure 3: Microscopic images on surface of Mg.

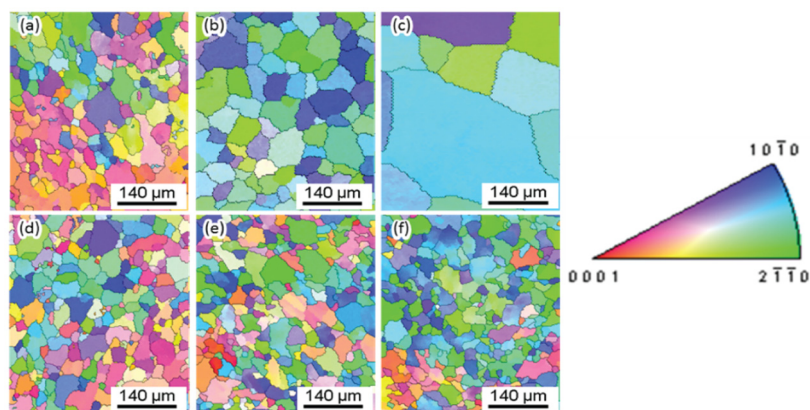


Figure 4: Inverse pole figure map of surface of Mg.

have higher value of Vickers hardness. From figure (a), (d), (e) and (f), Vickers hardness of the subsequent aged samples was slightly decreased as the aging time increases the Vickers hardness decreases. Based on grain observation in optical microscope and EBSD, there is no change in grain size of the ECAP sample and the subsequent aged sample. Accordingly, It was considered that the Vickers hardness of the subsequent aged samples were reduced by the recovery of crystal defects in the heat treatment below the recrystallization temperature.

3.3 Corrosion Behaviour in Constant Immersion Test

Constant immersion test is a more direct and illustrative approach to detect corrosion behaviour of a material. Fig.7 shows the mass loss of the ECAPed, the as-received, the annealed and the subsequent aging for 2, 4 and 6 hours pure Mg samples after 168 hours (7 days) immersed in RPMI 1640 medium. From Fig.7, it is obvious result that the ECAP sample has the largest mass loss in these conditions. Additionally, it shows the annealed sample has the most favourable corrosion resistance among the samples. From the both results of the grain size observation and the mass loss, during the corrosion test of the pure Mg in RPMI 1640 medium, there is no significant effect in grain size, however, it could be suggested that the other corrosion factor has remarkable effect. Furthermore, the corrosion resistance of the subsequent samples was improved as the heat treatment time increased.

Some researchers have reported that the corrosion resistance of materials have been improved by grain refinement which has been decreasing general corrosion rate and alleviating

corrosion localization (Janecek, 2005). Also, the better corrosion resistance of ECAPed Copper (Cu), Titanium (Ti) and industrial pure Aluminium (Al) with deformed microstructures than the coarse grains one have been indicated (Blyanov, 2004). However, unexpectedly, the ECAP process might weaken the corrosion resistance of the pure Mg. It could be considered that many crystal defects yielded by ECAP process reduced the corrosion resistance. It was considered that this negative phenomenon was related to the microstructure characterization and the corrosion mechanism of ECAPed pure Mg. It has been verified that the corrosion has been caused primarily by surface defects such as grain boundaries and dislocations (Aust, 1994).

The above results have demonstrated that the strain-induced crystalline defects are unfavourable for the corrosion resistance of pure Mg. However the corrosion behaviour of ECAPed pure Mg could be improved by subsequent annealing process.

Fig.8(a)–(f) shows the pH value. The pH value in all conditions was increased for approximately over 0-12 hours and decreased over 12-24 hours. After 24 hours, the pH value was slightly decreased. This tendency was particularly remarkable in the pure Mg ECAPed sample and the subsequent aging for 2, 4 and 6 hours samples. In this result, FBS was not added to the RPMI 1640 medium. There is a need to investigate the pH level in the case of enhancing the buffer function of the medium from now on. The rapid increase in the pH of the early stage of immersion test has not been sufficiently examined in the present study.

Fig.9 shows the amount of gas generated the ECAPed and the as-received sample after immersion for 24 hours. The amount of gas generated of the ECAPed sample was 1.72 ml/cm², the as-received

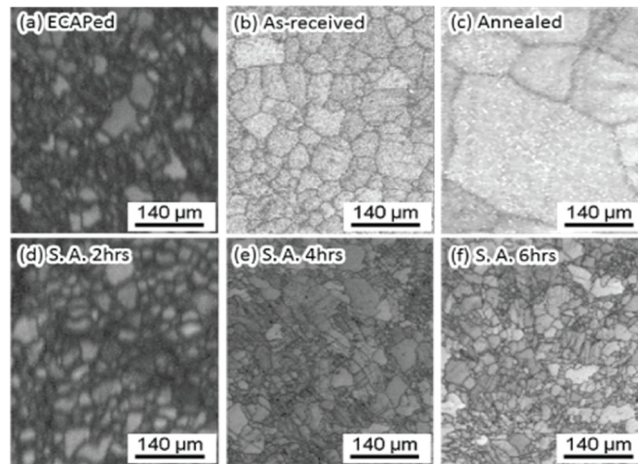


Figure 5: Image quality map on surface of Mg.

sample was 1.28 ml/cm². The ratio on gas generation volume of the as-received sample and the ECAPed sample were similar to the ratio on the mass loss of the as-received sample and the ECAPed sample. Therefore, it was suggested that there is a correlation between the amount of mass loss and the amount of gas generation.

Fig.10 shows the corroded surface of the ECAPed sample after immersion test for 24 hours by SEM. The Localized corrosion products could be observed on the sample surface. Fig.11 shows the result of the chemical element analysis in the same microscopic field by EDS. From the result, the main component elements of the corrosion products present in the sample surface were oxygen O, phosphorus P and calcium Ca. It could be assumed that the chemical compound produced on sample surface during the corrosion of pure magnesium in RPMI 1640 medium was a type of calcium phosphate. The peak of hydrogen of the light metal could not be detected by EDS.

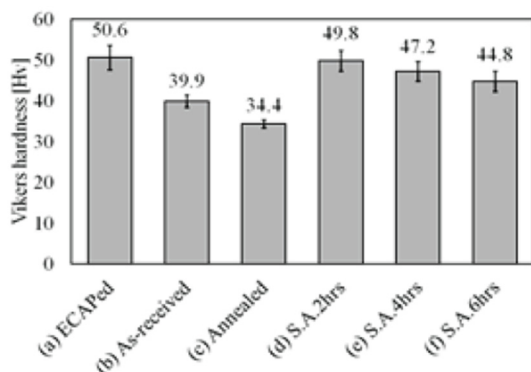


Figure 6: Vickers hardness test results.

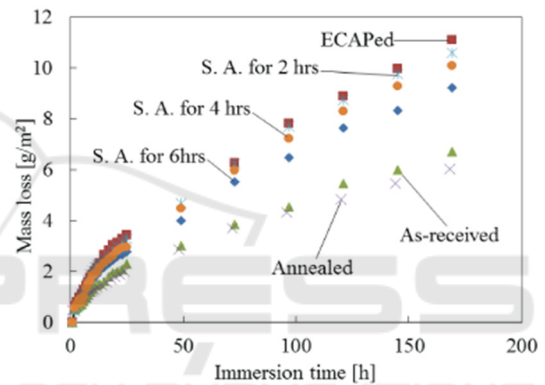


Figure 7: Relationship between mass loss and immersion time.

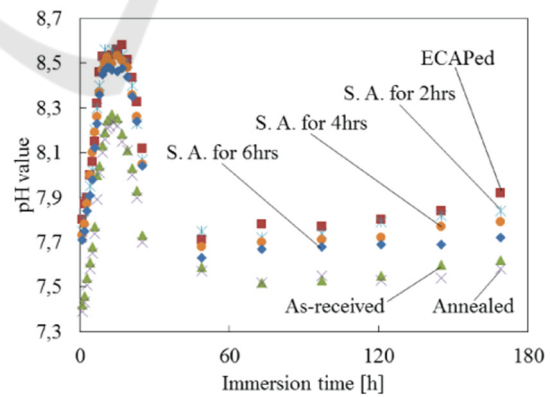


Figure 8: Relationship between pH and Immersion time.

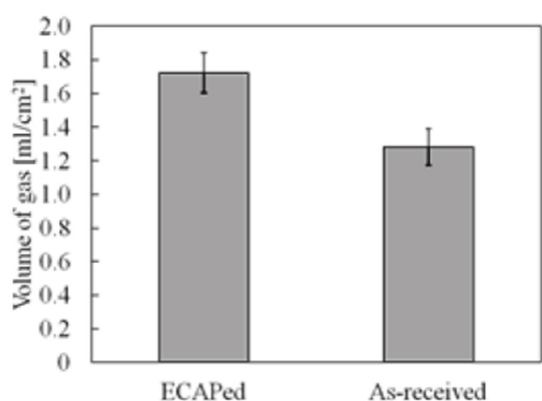


Figure 9: Volume of gas generation on ECAPed and As-received Mg.

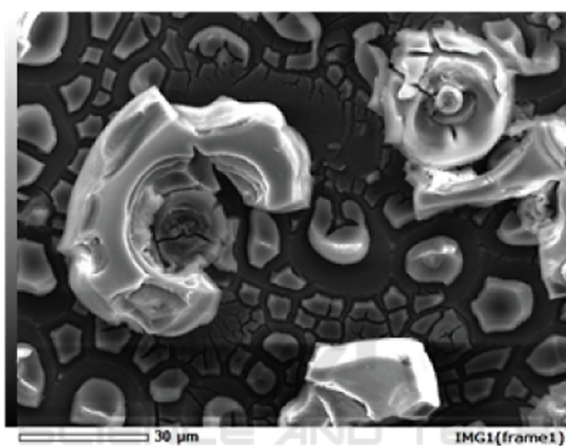


Figure 10: SEM image of ECAPed pure Mg sample after immersional test.

4 CONCLUSIONS

Fine grained pure Mg could be manufactured through the ECAP process at 573K. Also, the

subsequent annealing process below the re-crystallization temperature was applied by using the ECAPed samples in order to verify the effect of crystalline defects on weakening corrosion resistance of pure Mg without increasing grain sizes. The effect of microstructure on the corrosion behavior of the ECAPed pure Mg was investigated by optical microscopy and SEM observation, microhardness test and certain period immersion tests in RPMI 1640 medium.

(1) The difference in the microstructure by ECAP processing was observed by optical microscope and SEM with EBSD. The average grain size of ECAPed samples (30μm) were greatly reduced compared with the annealed sample (200μm). From the result of EBSD, the crystal orientation of ECAPed sample in comparison with the as-received and the annealed sample has significantly changed. The ECAPed sample was found to be less crystalline alongside of the as-received and the annealed sample. It could be considered that the crystal defects of the material by introducing a shear strain to the material have been increased by ECAP process. In addition, it has been confirmed that crystal defects such as dislocation and strain of ECAPed sample was recovered by subsequent aging.

(2) The corrosion behaviour of the ECAPed pure Mg was investigated by the immersion test for certain period. From the results of the immersion test, it has been revealed that the corrosion resistance of pure Mg in RPMI 1640 medium has been reduced ECAP process. The strain-induced crystalline defects were unfavourable for the corrosion resistance of pure Mg. However, the corrosion resistance of ECAPed pure Mg could be improved by subsequent aging process. On the other hand, the ratio on gas generation volume of the as-received sample and the ECAPed sample were similar to the ratio on the mass loss of the as-received sample and the ECAPed sample. Therefore, it was suggested

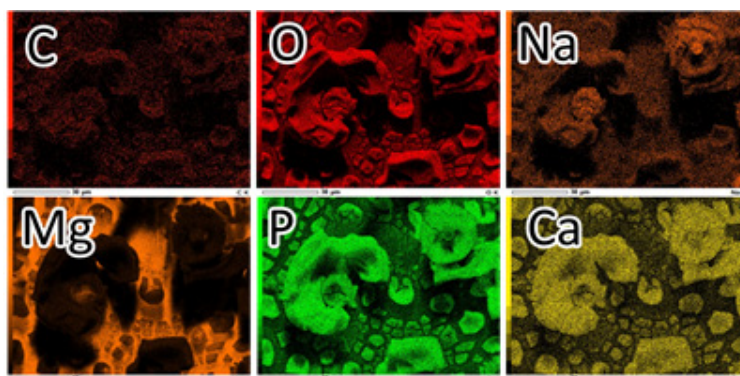


Figure 11: EDS images of ECAPed pure Mg sample after immersion test.

that there is a correlation between the amount of mass loss and the amount of gas generation. (3) The surface of the ECAPed sample after the immersion test for 24 hours was observed to identify the corrosion products by EDS. The localized corrosion products were observed on the sample surface. Then, from the result, it could be assumed that the chemical compound which has been produced on sample surface during the corrosion of pure magnesium in RPMI 1640 medium was a type of calcium phosphate.

- Werkhoven R. J., Sillekens W. H., J. B. J. M. van Lieshout, 2011. *Effect of surface roughness on the in vitro degradation behavior of a biodegradable magnesium-based alloy*, Magnesium Technology, pp. 419–422.
- C. S. Wu, Z. Zhang, F.H. Cao, L.J. Zhang, J.Q. Zhang, C.N. Cao, 2007. *Study on the anodizing of AZ31 magnesium alloys in alkaline borate solutions*, Appl. Surf. Sci., 253, pp. 3893–3898.
- L. Xu, G. Yu, E. Zhang, F. Pan, K. Yang, 2007. *In vivo corrosion behavior of Mg–Mn–Zn alloy for bone implant application*, J. Biomed. Mater. Res. A., 83, pp. 703–711.

ACKNOWLEDGEMENTS

This work was supported by JSPS KAKENHI Grant Numbers JP16K05974, JP25420010.

REFERENCES

- K. T. Aust, U. Erb, G. Palumbo, 1994. *Interface control for resistance to intergranular cracking*, Mater. Sci. Eng. A, 176, pp. 329–334.
- A. Blyanov, J. Kutnyakova, N.A. Amirkhanova, V.V. Stolyarov, R.Z. Valiev, X.Z. Liao, Y.H. Zhao, Y.B. Jiang, H.F. Xu, T.C. Lowe, Y.T. Zhu, 2004. *Corrosion resistance of ultra fine-grained Ti*, Scr. Mater., 51, pp. 225–229.
- Hiromoto, S., 2014. *Corrosion behavior of magnesium alloys for biomaterial use*, Corrosion engineering of Japan, 63, pp. 371–377.
- Jae Yeol Park, Dong Nyung Lee, 2008. *Deformation and annealing textures of equal-channel angular pressed 1050 Al alloys strips*, Mater. Sci. Eng. A, 497, pp. 395–407.
- M. Janecek, B. Hadzima, R.J. Hellmig, Y. Estrin, 2005. *The influence of microstructure on the corrosion properties of Cu polycrystals prepared by ECAP*, Metall. Mater., 43, pp. 258–271.
- A. Loos, R. Rohde, A. Haverich, S. Barlach, 2007. *In vitro and in vivo biocompatibility testing of absorbable metal stents*, Macromol. Symp., 253, pp. 103–108.
- G. Mani, M.D. Feldman, D. Patel, C.M. Agrawal, 2007. *Coronary stents: a materials perspective*, Biomaterials, 28, pp. 1689–1710.
- Raila, B., Anne, S., Stefanie R., Simon W., Mathias B., Svea P., Stephan F., Katrin S., 2014. *New stent surface materials: The impact of polymer-dependent interactions of human endothelial cells, smooth muscle cells, and platelets*, Acta Biomaterialia, 10, pp. 688–700.
- Dan Song, AiBin Ma, , Jinghua Jiang, Pinghua Lin, Donghui Yang, Junfeng Fan, Jung-Gu Kim, 2010. *Corrosion behavior of equal-channel-angular-pressed pure magnesium in NaCl aqueous solution*, Corrosion Science, 52, pp. 481–490.